

Skyrmions in layered anti-ferromagnetic materials

Stability of skyrmion crystals in
transition-metal dihalides

Joeri Vendrik (s2370255)

July 6, 2017

Abstract

Magnetic skyrmions are topologically protected spin textures with great perspective in the field of magnetic processing devices and information storage. They are experimentally observed in chiral magnets and are also theoretically predicted for frustrated magnets. In this research, spiral states in a frustrated magnet, $NiBr_2$, are investigated to find the skyrmion crystal. A six layer model is used with ferromagnetic nearest-neighbor interactions, anti-ferromagnetic next-nearest neighbor and interlayer interactions, uniaxial anisotropy and an external magnetic field. A magnetic phase diagram is produced for varying strength of the coupling between the layers and the external magnetic field. Furthermore, an attempt is made to explain this diagram qualitatively.

Contents

1	Introduction	2
2	Theory	4
2.1	General properties of skyrmions	4
2.2	Skyrmions in chiral magnets	6
2.3	Skyrmions in frustrated magnets	7
2.3.1	Frustrated magnets	8
2.3.2	Interactions	8
2.3.3	Stability of skyrmions in frustrated magnets	9
2.4	Landau-Liftshitz-Gilbert equation	10
2.5	Phase transitions	10
2.6	Electromagnetic properties	11
2.7	Technological applications	12
3	Results	14
3.1	The model	14
3.2	Phase diagram	15
3.2.1	States	17
3.2.2	Phase transitions	18
4	Discussion and Conclusion	20
4.1	Discussion	20
4.2	Conclusion	21
5	Appendix	23
5.1	Appendix A: derivation of Landau-Liftshitz-Gilbert equation	23
5.2	Appendix B: Results	24
5.3	Appendix C: Phasediagrams of two and six layer model	25
5.4	Appendix D: Abbreviations	26

1 Introduction

In field theory, particles are presented as excitations of the field. This means that they have a higher energy and more momentum than the ground state. The fact that particles have a higher energy than the ground state would suggest that they have a finite lifetime or in other words: they are not stable. However, the opposite turns out to be true. One possible explanation for this problem was given by the physicist Skyrme, who argued that particles are characterized by a topological value which can not be changed by a continuous deformation of the field. Even though his theory did not become the prevailing explanation for the stability of particles, it is still useful since it can be used for the description of topologically protected spin textures which were discovered in several kind of magnetic systems. These protected spin textures are appropriately called skyrmions.[1] They can exist as a skyrmion crystal (SkX) or as isolated skyrmions.

Spiral states, like skyrmions, are stabilized by competing interactions and exist in several kinds of magnetic systems. In non-centrosymmetric, or chiral, ferromagnets the skyrmions are produced by competing exchange and Dzyaloshinskii–Moriya interactions. In magnetic thin films with easy-axis anisotropy, they arise because of the competition between dipole-dipole interactions and the anisotropy interaction. And at last, in frustrated magnets skyrmions are stabilized by competing ferromagnetic and antiferromagnetic exchange interactions. Since the skyrmions in these systems are stabilized with different mechanisms, their properties also differ. More on these differences will follow in the theory part.

Skyrmions were predicted theoretically, but it took a long time before they were observed experimentally. With the use of small-angle neutron scattering, it was shown that the spin structure of the A-phase of MnSi, which was unspecified up till then, corresponds to the skyrmion crystal.[2] Small-angle neutron scattering pictures the reciprocal space, which is the Fourier transform of the phase. In the case of the skyrmion crystal this shows a hexagon with the norm of the wave vectors in the plane perpendicular to the \mathbf{k} -vector of the incident neutrons, while for other magnetic structures there is no patterns in this plane.[1]

It is also possible to observe skyrmion crystals in real space. Several techniques used to investigate them in real space are magnetic force microscopy, spin-polarized scanning tunneling microscopy and Lorentz transmission electron microscopy, from now on called LTEM(all abbreviations are given in appendix D). The most suitable one is LTEM, since it has nanometer resolution and works well with a perpendicular magnetic field. With this method, an electron beam transmits a thin slice of the material, just as is the case with a regular transmission electron microscope. These electrons are deflected by the Lorentz force caused by the magnetic field, which is caused by the magnetization of the material, and as a consequence the magnetization of the material can be mapped by looking at this deflection. Experimental phase diagrams have been produced for several materials by using this technique.

Magnetic skyrmions generate a great deal of interest, because they have

certain properties that make them excellent candidates for magnetic information storage. One of these properties is their flexibility, which makes sure they are hardly affected by impurities of the material. Furthermore, the current-density needed to de-pin them is very low in comparison with other magnetic structures like domain walls.

One of possibilities to use skyrmions in magnetic information storage is creating a type of computer memory which resembles the magnetic bubble memory. These were produced in the 1970's and 1980's, but disappeared when faster semi-conductor memory chips made an appearance. [3] However, skyrmions are way smaller than magnetic bubbles, so skyrmion-based memory would have a much larger information density. In this kind of device, each skyrmion stores 1 bit of information.

Another option is using the skyrmion in race-track memory. Race-track memory is already used with domain walls, but using skyrmions would cost way less energy because of the lower de-pinning current needed. In race-track memory, the information is stored in the form of skyrmions in 'racetracks', which would be nanowires or nanostripes.[4] More on the technological possibilities of skyrmions will follow in section 2.7.

The technological options of skyrmions described above are the reason skyrmions are widely investigated. As mentioned above, skyrmions have been observed experimentally in chiral magnets. But this is not the case for frustrated magnets, where they have only been predicted theoretically recently. More research has to be done on skyrmions in frustrated magnets, in order for this to happen.

In this paper an attempt is made to find the SkX-phase in $NiBr_2$. A model of this material is made with six layers of triangular lattices, which are antiferromagnetically coupled and shifted with respect to each other. This kind model is used since $NiBr_2$ has a unit cell of 3 layers with ABC stacking. The in-plane nearest neighbors are ferromagnetically coupled and the in-plane next nearest neighbors antiferromagnetically. Finally, an external magnetic field is applied in the same direction as the uniaxial anisotropy.

These interactions can lead to several spiral states like the conical spiral, the vertical spiral, the 2q-state and the skyrmion phase. Phase transitions between these states can be both first and second order.

The magnetic states are investigated by varying the strength of the inter-layer anti-ferromagnetic coupling and the strength of the external magnetic field and the main goal is to find the skyrmion phase. A magnetic phase diagram is generated and an attempt is made to give a qualitative explanation why certain phase transitions occur.

2 Theory

2.1 General properties of skyrmions

Magnetic skyrmions are complex non-coplanar spin-structures which are topologically non-trivial. The fact that they are topologically non-trivial gives them a long lifetime, since they cannot continuously transform into topologically trivial structures like ferromagnets. In other words: skyrmions have a certain invariant measure, called the topological skyrmion number. The topological skyrmion number measures how many times you can wrap the spins around a sphere and is given by the following formula:

$$N = \frac{1}{4\pi} \int \int d^2\mathbf{r} \left(\frac{d\mathbf{n}}{dx} \times \frac{d\mathbf{n}}{dy} \right) \cdot \mathbf{n} \quad (1)$$

where $\mathbf{n}(\mathbf{r})$ indicates the direction of the spin at position $\mathbf{r} = (x, y)$.

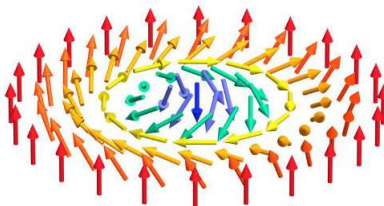


Figure 1: Isolated skyrmion

Skyrmions can exist in the form of a crystal in a phase called the SkX-phase, which is shown below. But it is also possible to stabilize isolated skyrmions under certain circumstances. These isolated skyrmions are expected to have more practical use than skyrmion crystals.[5]

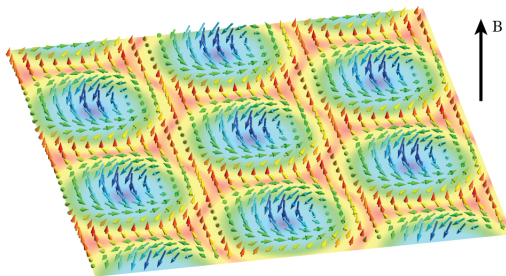


Figure 2: Skyrmion crystal(SkX).

Exotic spin-structures like skyrmions, but also other spiral states, can arise in both chiral magnets and frustrated magnets. In both cases competing interactions which favor a different spin direction are the cause of the spiral states,

but the interactions are different. In chiral magnets the competition between the ferromagnetic (FM) interaction and the Dzyaloshinskii-Moriya (DM) interaction is the key factor in stabilizing skyrmion states, while in frustrated magnets competing ferromagnetic and anti-ferromagnetic exchange interactions are the reason spiral states are stabilized. In this paper skyrmions in frustrated magnets with uniaxial anisotropy are investigated. But both cases will be discussed in section 2.2 and 2.3.

Skyrmions can have different possible patterns, which are defined by two values: the vorticity, m and the helicity, γ . These values appear when the direction of the spin, $\mathbf{m}(\mathbf{r})$, is expressed in spherical coordinates. They determine the azimuthal angle Φ of m :

$$\Phi(\phi) = m\phi + \gamma \quad (2)$$

in which the angle ϕ is the azimuthal angle of \mathbf{r} . It can be shown that the vorticity is equal to the skyrmion number N . The vorticity and the helicity will have the value which gives the lowest energy.

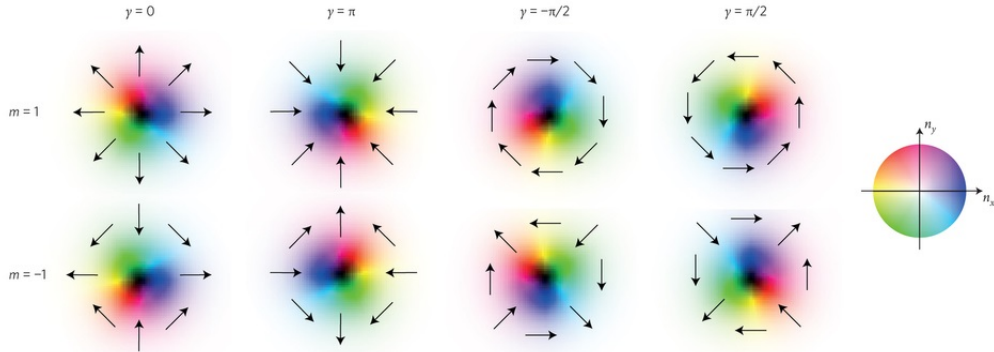


Figure 3: In this figure skyrmion structures for different values of the vorticity and helicity are shown. In this figure the arrows indicate the in-plane directions of the spins and the colors indicate the direction of the spin perpendicular to the plane.

2.2 Skyrmions in chiral magnets

Magnets are called chiral if their atomic structure lacks inversion-symmetry. The Dzyaloshinskii-Moriya interaction, from now on called the DM interaction, is only active in these kind of systems and is caused by spin-orbit coupling. It is the reason spiral states appear in these kinds of magnets. In the case of two neighboring atoms the Hamiltonian of the DM interaction is given by

$$H_{DM} = -\mathbf{D}_{ij} \cdot (\mathbf{S}_i \times \mathbf{S}_j) \quad (3)$$

In this equation \mathbf{S}_i and \mathbf{S}_j indicate the spins of the neighboring atoms and \mathbf{D}_{12} is the DM interaction vector.[6] The direction of this vector depends on the direction in which the inversion-symmetry is broken and the magnitude depends on the strength of the spin-orbit coupling.

The direct result of the competition between the DM and the FM interaction is canting of the spins. The DM interaction prefers an angle of $\frac{\pi}{2}$ between neighboring spins, while the FM interaction prefers alignment. This leads to tilting of the spins by a small angle with respect to the collinear configuration. This canting can have two possible macroscopic results. It can either lead to a weaker ferromagnetic state or to spiral states. [7]

In the theory of phase transitions proposed by Landau the transitions are evaluated by considering a phenomenological expression of the free energy near the transition point. This free energy is written down as a Taylor expansion in the order parameter, which defines the degree of order at the phase-transition.[8] It can be shown that the free energy term caused by the DM interaction has the following form:

$$F_l = \mathbf{D} \cdot [\mathbf{m}(\nabla \cdot \mathbf{m}) - (\mathbf{m} \cdot \nabla)\mathbf{m}] \quad (4)$$

In this formula \mathbf{m} is the order parameter and \mathbf{D} is the DM interaction vector. Terms of this form, with linear terms of the order parameter and its gradient, are called Lifshitz invariants and are the reason instabilities in the order parameter can develop. In this case, these instabilities lead to spiral states. [9]

However, not all spiral states are skyrmionic. To investigate the stability of skyrmions in chiral magnets, one of the most well-known examples is used: MnSi. As mentioned before, this was the material in which the first skyrmions were discovered experimentally.

In MnSi, the competition of the DM interaction with ferromagnetic and Zeeman interactions leads to a helical ground state with a single wave vector at zero temperature and a small magnetic field. It goes to a conical phase as the magnetic field is increased, since it obtains a component parallel to magnetic field. However for certain values of H and T, a skyrmion phase can be stabilized. This usually occurs close to the Curie temperature, T_c , at which the transition between ordered and paramagnetic states occurs. The stability of the skyrmion at this region can be explained by studying the Ginzburg-Landau free energy function near T_c . [3] It can be shown that a skyrmion phase always has a higher energy than the conical phase if only ferromagnetic, DM and Zeeman interactions are considered. However, if thermal fluctuations are included, the skyrmion

crystal becomes stable in a small region near T_c . The precedent can be seen in the phase diagram of MnSi below. Anisotropies can also be included, but it turns out that it does not have a large influence on the stability of skyrmions.

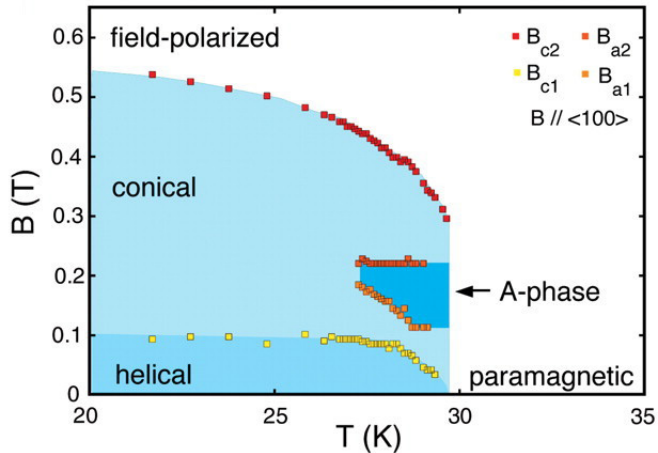


Figure 4: phase diagram MnSi. The A-phase in the diagram is the skyrmion phase.

The size of these spiral structures depend on the ratio between the DM interaction and the ferromagnetic interaction. It can be shown that $\frac{D}{\sqrt{2}J} = \tan(\frac{2\pi}{\lambda})$, where λ is the wavelength of the structure in units of the lattice constant. The wavelength of skyrmions produced by this mechanism is usually of the order of 5-100nm.

2.3 Skyrmions in frustrated magnets

In this paper skyrmions in frustrated magnets with uniaxial anisotropy are investigated. While in chiral magnets spiral states can only be stabilized by competing FM and DM interaction, in frustrated magnets these states can only occur in the case of competing exchange interactions. These interactions do not depend on the direction of the spin rotation, in contrast to the DM interaction. As was mentioned before, the vorticity and helicity take the values that give the lowest energy. In the case of the DM interaction, the lowest energy is obtained when $m = 1$ and $\gamma = \pm\pi$. The sign of γ depends on the direction of the DM interaction. In the case of the frustrated magnet both $m = 1$ and $m = -1$ give the same energy and the energy does not depend on γ , so it can take any arbitrary value. This is reason that skyrmions in frustrated magnets have 2 extra degrees of freedom with respect to the skyrmions in chiral magnets. Both skyrmions and anti-skyrmions, which have vorticity -1, can coexist in frustrated magnets. More on frustrated magnets in general, the interactions and the stability of skyrmions in these magnets will follow now.

2.3.1 Frustrated magnets

Frustrated magnets are a form of geometric frustration that occurs in anti-ferromagnets with certain kind of lattice structure, like a triangular lattice. The frustration arises because every spin wants to be anti-parallel to its neighbor, but this is impossible in a triangular lattice. In a triangle two spins can be anti-parallel, but the third one can't be anti-parallel to them both. This means that there are six possibilities for the configuration of the three spins, all with the same energy. This is visualized in the figure below.

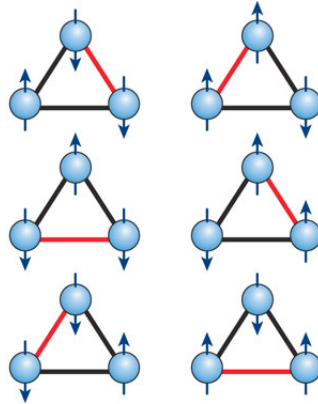


Figure 5: Visualization of frustration in triangles.

In the example above, there were only 3 spins to consider and there were already 6 degenerate states. If the size of the system increases, the number of equal energy states will also increase. This leads to a significantly large entropy, since the entropy of a system is proportional to the logarithm of the available states according to Boltzmann's equation.[10]

Frustration can be expressed best in terms of the magnetic susceptibility, χ , which is defined as the response of a magnetic material to an external field $M = \chi H$, with M the magnetization of the material and H the external field. AFM materials will go to its ordered state below a certain temperature, called the Curie-temperature, at which the thermal fluctuation no longer disturb the ordering. The Curie-temperature depends on the material. In the AFM state the susceptibility of the material is zero. However, in frustrated magnets this ordering is suppressed and there won't be an ordered state, even at very low temperatures.

2.3.2 Interactions

As was mentioned before, in this paper skyrmions arising from competing exchange interactions in frustrated magnets are investigated. These exchange interactions, described by Heisenberg, are described by the following Hamilto-

nian:

$$H = - \sum_{ij} J_{ex}(\mathbf{r}_{ij}) \mathbf{S}_i \cdot \mathbf{S}_j \quad (5)$$

$J_{ex}(\mathbf{r}_{ij})$ is called the exchange constant and depends on the overlap of the electronic states of the atoms labeled with i and j . Clearly this overlap depends on the distance and angle between the two atoms. This constant can be both positive or negative, if it is negative you get AFM interactions, since you get the lowest energy when neighboring spins are opposite and if it is positive you get FM interactions since the lowest energy is obtained when spins align.

Furthermore Zeeman-energy and anisotropy energy are taken into account. The Hamiltonian of the Zeeman term is given by

$$H = - \sum_i \mathbf{B} \cdot \mu_i \quad (6)$$

where μ_i is the atomic magnetic moment which is proportional to the spin of the atom and \mathbf{B} is the external magnetic field.

Most of the materials are not isotropic, so the magnetization has a preferential direction. In the case of the triangular lattice there is an uniaxial anisotropy, which means the magnetization wants to point into one certain direction, called the easy-axis. When the easy-axis is in the z-direction, the Hamiltonian is the following

$$H = -K \sum_i (S_i^z)^2 \quad (7)$$

where \mathbf{K} points in the direction of the easy-axis and has its value is the anisotropy parameter. It can easily seen that opposing spins give the same energy. This can be explained by the fact that the easy-axis points in both directions.

The total Hamiltonian becomes:

$$H = - \sum_{AFM, FM} \sum_{ij} J_{ex}(\mathbf{r}_{ij}) \mathbf{S}_i \cdot \mathbf{S}_j - \sum_i \mathbf{B} \cdot \mu_i - K \sum_i (S_i^z)^2 \quad (8)$$

2.3.3 Stability of skyrmions in frustrated magnets

As was mentioned before, the stability of skyrmion in frustrated magnets is the topic of this paper and will be researched by the use of a model. But just as was the case with chiral magnets, not all frustrated magnets with competing ferromagnetic and anti-ferromagnetic coupling have spiral magnetic states to begin with. It can be shown that the ratio of the absolute values of the exchange constants $\frac{J_1}{J_2}$ has to be larger than 1/3, where J_1 and J_2 are the exchange constant for the ferromagnetic and the anti-ferromagnetic interaction. [11]

Just as with chiral magnets, the size of the spiral structures depends on the ratio between the competing interactions. In this case it depends mostly on the ratio between J_1 and J_2 . It also depends on the other interactions, but their contributions are negligible. It can be shown that

$$\cos\left(\frac{\sqrt{3}Q}{2}\right) = \frac{J_1 - J_2}{2J_2} \quad (9)$$

In this formula $Q = \frac{2\pi}{\lambda}$, where λ is the wavelength of the structure in units of the lattice constant. The wavelengths of these skyrmions are usually smaller than the ones in chiral magnets. They are of the order of a few nanometer while the ones in chiral magnets are of the order of 5-100nm.

2.4 Landau-Liftshitz-Gilbert equation

The Landau-Liftshitz-Gilbert (LLG) equation is a differential equation which can be used to describe the dynamics of several physical systems.[12] It was derived by Landau and Liftshitz based on the interactions which can influence the magnetic structure. Gilbert added a damping term to compensate for the saturation magnetization, which is the maximal value of the magnetization reached when the ferromagnetic state is reached and all spins align. In this paper this equation will be used to determine the evolution of the spin configuration. The LLG-equation can have various forms and the form that will be used in this paper is the following:

$$\dot{\mathbf{S}} = -\frac{1}{1+\alpha^2}\mathbf{S} \times \mathbf{H}^{\text{eff}} - \frac{\alpha}{1+\alpha^2}\mathbf{S} \times \dot{\mathbf{S}} \times \mathbf{H}^{\text{eff}} \quad (10)$$

The \mathbf{H}^{eff} term is called the effective field and the α term is called the Gilbert-damping. The derivation of the LLG-equation is done in appendix A by considering a one electron system with an external magnetic field.

The effective field is the local field felt by the magnetization. So, the Hamiltonian can be determined by considering the Zeeman energy and replacing the magnetic field by the effective field

$$H = -\mathbf{H}^{\text{eff}} \cdot \boldsymbol{\mu} \quad (11)$$

or equivalently:

$$\mathbf{H}^{\text{eff}} = -\gamma \frac{\delta H}{\delta \mathbf{S}} \quad (12)$$

where $\gamma = \frac{\mu}{S}$.

2.5 Phase transitions

As was mentioned in the introduction, phase-transitions occur between the magnetic phases. The phase-transitions can be both first and second order and these transitions have different physical properties, so they are determined in a different way.

In the theory of phase transitions proposed by Landau the transitions are evaluated by considering a phenomenological expression of the free energy near the transition point. [8] This free energy is written down as a Taylor expansion in the order parameter, which defines the degree of order at the phase-transition.

First order transitions have a discontinuity in the first derivative of the free energy, while second order transitions, are continuous in the first derivative but discontinuous in higher derivatives. Other names for these transitions are

discontinuous and continuous transitions. According to this theory, higher-than-second-order transitions can occur, but these won't be regarded.

In second order transitions the order parameter is continuous across the transition, so the expansion technique of Landau can be used legitimately. The parameter is zero in one phase and non-zero in the other phase, so the transition can be found by regarding the order parameter with respect to the varying magnitude of the interaction.

In first order transitions, the order parameter is not continuous over the transition, so this technique cannot be used and only the fact that the free energy of both states is equal at the transition can be used.

2.6 Electromagnetic properties

When spin-structures like skyrmions, but also helical or conical states, couple to electrons, some particular phenomena take place. These phenomena are the reason skyrmions are so interesting so they will be discussed here.

One of the phenomena is the emergence of effective electric and magnetic fields. The magnetization acts on the conduction electrons by coupling of the spins of conduction electrons to the spins of the lattice atoms. The assumption is made that this coupling is sufficiently strong to make sure that the spin of the conduction electron points in the same direction as the local magnetization of the skyrmion and follows the variations of this magnetization instantaneously.

This coupling can be described by considering the Schrödinger equation of the conduction electron:

$$i \frac{\partial}{\partial t} \Psi(\mathbf{r}) = \left[\frac{p^2}{2m_e} - J_{ex} \sigma \cdot \mathbf{m}(\mathbf{r}) \right] \Psi(\mathbf{r}) \quad (13)$$

The spin of the conduction electron is represented by σ and the spin of the lattice atoms at position \mathbf{r} is given by $\mathbf{m}(\mathbf{r})$. $\psi(\mathbf{r})$ is the wavefunction of the electron. To determine the effect of this coupling, the quantization axis \mathbf{e}_z is rotated to point in the direction of $\mathbf{m}(\mathbf{r}, t)$ by the operator $U(\mathbf{r}, t) = \exp(i\frac{\theta}{2}\sigma \cdot \mathbf{n})$, with θ the angle of reflection and \mathbf{n} the rotation axis, defined as $\mathbf{n} = \frac{\mathbf{n} \times \mathbf{e}_z}{|\mathbf{n} \times \mathbf{e}_z|}$. Now formula 13 can be rewritten as:

$$i\hbar \frac{\partial}{\partial t} \phi = \left[\frac{(\mathbf{p} + e\mathbf{A})^2}{2m_e} - 2J_{ex} \sigma_z - eV \right] \phi \quad (14)$$

with $\Psi = U(\mathbf{r}, t)\phi$. \mathbf{A} is the vector potential and is defined as $\mathbf{A} = -\frac{i\hbar}{e} U^\dagger \Delta U$ and V is the scalar potential defined as $V = \frac{i\hbar}{e} U^\dagger \partial_t U$. The vector potential and the scalar potential are small perturbations of the unperturbed Hamiltonian in formula 13.

These potentials give rise to an emergent electric field and an emergent magnetic field. The electric field is given by

$$E_i^{em} = -\partial_i V - \partial_t A = \frac{\hbar}{e} \mathbf{m} \cdot (\partial_i \mathbf{m} \times \partial_t \mathbf{m}) \quad (15)$$

The emergent magnetic field is given by

$$B_i^{em} = \epsilon_{ijk}(\partial_j A_k - \partial_k A_j) = \frac{\hbar}{2e} \epsilon_{ijk} \mathbf{m} \cdot (\partial_j \mathbf{m} \times \partial_k \mathbf{m}) \quad (16)$$

In both formulas i,j and k indicate the space coordinates and ϵ_{ijk} is the Levi-Civita tensor.

With the help of formula 1, it can be shown that the magnetic flux is the following:

$$\Phi = \int \mathbf{B}^{em} dx dy = -4\pi \frac{\hbar}{2e} = -\frac{h}{4e} \quad (17)$$

The emergent magnetic field gives rise to a Hall effect acting on the conduction electrons, called the topological Hall effect. This can be shown by considering the Lorentz-force

$$\mathbf{F} = -e(\mathbf{E}^{ex} + \mathbf{E}^{em}) - e(\mathbf{v}_e - \mathbf{v}_{skyrm}) \times (\mathbf{B}^{ex} + \mathbf{B}^{em}) \quad (18)$$

The $-e(\mathbf{v}_{skyrm} \times \mathbf{B}^{em})$ term and the $-e\mathbf{E}^{em}$ term cancel because of Faraday's law. So the resulting force acting on the conduction electron, caused by the emergent electric- and magnetic field, is $-e(\mathbf{v}_e \times \mathbf{B}^{em})$. This phenomenon is called the topological Hall effect. It was because of this effect that it was shown that the a-phase in MnSi, as seen in figure 2, was actually the skyrmion crystal phase.[2] This happened by small-angle neutron scattering, as was already mentioned in the introduction.

2.7 Technological applications

The main technological benefits of skyrmions are caused by their peculiar dynamics when external electric fields are applied. The first advantage of skyrmions is their independence of impurities. While for other magnetic materials the velocity decreases when the amount of impurities is raised, it remains constant for skyrmions. This is caused by the flexibility of their structure and their particle-like behavior.[3] It is easier to deform a triangular shape, which a skyrmion crystal has.

Furthermore, the motion of the skyrmions barely depend on the Gilbert damping and the non-adiabatic effect. To show this, Thiele's equation has to be considered, which describes the centre-of-mass motion of spin-structures.[3]

$$\mathbf{G} \times (\mathbf{v}_e - \mathbf{v}_{skyrm}) + \kappa(\alpha \mathbf{v}_{skyrm} - \beta \mathbf{v}_e) + M_{skyrm} \frac{d\mathbf{v}_{skyrm}}{dt} = -\Delta U \quad (19)$$

In this equation α is the Gilbert-damping, introduced before, β is a non-adiabatic term, and U is a potential caused by impurities and boundary effects. \mathbf{G} is the gyromagnetic coupling vector and can be shown to be $\mathbf{G} = 4\pi N \mathbf{e}_z$, with N the skyrmion number. For other magnetic structures, like domain-walls or helical structures, this value is zero.

The Gilbert-damping term, α , and the non-adiabatic term, β , are both of the order 10^{-2} , so they can be neglected in the case of the skyrmion because the gyromagnetic coupling vector is multiple orders of magnitude larger.

This leads to the following expression for skyrmions: $\mathbf{G} \times (\mathbf{v}_e - \mathbf{v}_{\text{skyrm}}) \sim -\Delta U$, which means that the motion of the Skyrmion barely depend on α and β , as for other magnetic structures with $\mathbf{G} = 0$ the following relation applies $(\alpha \mathbf{v}_{\text{skyrm}} - \beta \mathbf{v}_e) \sim -\Delta U$. This leads to $\mathbf{v}_{\text{skyrm}} \sim \frac{\beta}{\alpha} \mathbf{v}_e - \Delta U$.

Furthermore it can be shown from Thiele's equation that the skyrmions also experience a Hall effect, called the Skyrmion Hall effect that lead to a transverse term of $\mathbf{v}_{\text{skyrm}}$ proportional to $(\alpha - \beta)$.

Apart from the fact that the velocity of the skyrmion is hardly affected by impurities, Gilbert-damping or the non-adiabatic effect, it has another advantage. The current-density needed to be able to de-pin domain walls is 10^{11} Am^{-2} , while this is only 10^6 Am^{-2} for skyrmions.

As was mentioned in the introduction, one of the possible devices is a skyrmion-based race-track memory, a model of this device is shown on figure 6. This device would have low-energy costs, ultra-high density and non-volatile memory, which means that information can be retrieved even if the device has been turned off. In race-track memory, an electric current is used to move magnetic structures, in this case skyrmions, so the lower de-pinning current is a mayor advantage in this step. After this, the skyrmions move past the writing elements which manipulates them to record patterns of bits which can be read by the reading element. The actual device would consist of many of these nanostripes. More research has to be done on the behavior of skyrmions to make it possible to actually produce them, [4]

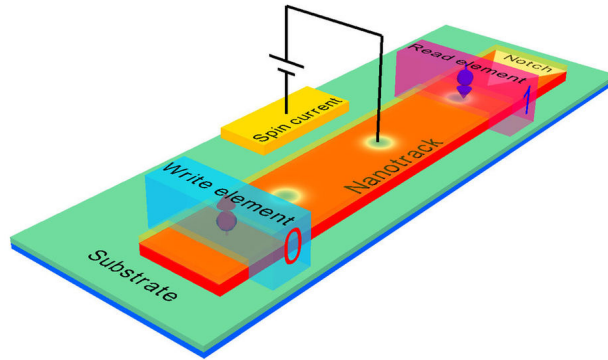


Figure 6: Skyrmion-based racetrack memory.

3 Results

3.1 The model

For the investigation of the skyrmions a model of six layers with triangular lattices, which are ABC stacked, is used. Six layers are used since the unit cell of $NiBr_2$ has three layers. If only three layers were used, the first and the third layer would have been ferromagnetically coupled, which is incorrect. Each layer consists of twelve by twelve atoms for reasons given later. Boundary conditions are added to couple the first and the sixth layer and to couple the edges of the layers. The crystal structure of the material is shown in the figure below.

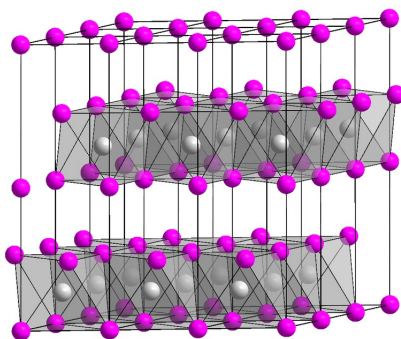


Figure 7: Crystal structure $NiBr_2$.

The material will go to the spin-configuration which gives the lowest total energy, so to determine this the Hamiltonian needs to be evaluated. As was mentioned before, the material is a frustrated magnet and the assumption is made that there is a FM-interaction between in-plane nearest-neighbors(NN) and an AFM-interaction between in-plane next-nearest-neighbors(NNN) and nearest-neighbors of the adjacent layers. The easy-axis of the material and the external magnetic field both point in the z-direction. With this information, the general Hamiltonian, given in formula 8, can be rewritten as follows

$$H = -J_1 \sum_{\langle ij \rangle, l} \mathbf{s}_i^l \cdot \mathbf{s}_j^l + J_2 \sum_{\langle\langle ij \rangle\rangle, l} \mathbf{s}_i^l \cdot \mathbf{s}_j^l + 2J_\perp \sum_{i, l} \mathbf{s}_i^{l_a} \cdot \mathbf{s}_i^{l_b} - K \sum_{i, l} (\mathbf{s}_{iz}^l)^2 - B \sum_{i, l} \mathbf{s}_{iz}^l \quad (20)$$

Here i and j indicate the points in a particular layer and l indicates the layer. J_1 , J_2 and J_\perp give the coupling constants for the FM and AFM interactions, K is the anisotropy term and B is value of the external magnetic field. The value of B is multiplied by $\frac{\mu}{S}$ in comparison with formula 8, to replace μ with S . J_1 is set to be 1. The value of J_2 is chosen in such a way that an integer amount of spiral structures fit in one layer and it has to be larger than 1/3 of course, because otherwise spiral states do not appear. To make this happen, formula 9 is used. The length of a spiral structure is related to the wavelength

by $a = \frac{2\lambda}{\sqrt{3}}$. After applying this, formula 9 can be rewritten to give

$$J_2 = (2\cos(\frac{\pi}{a}) + 1)^{-1} \quad (21)$$

J_2 is set to 0.5, so the size of the spirals are six. This is the reason the choice is made to have layers of twelve by twelve atoms.

As was mentioned before, the spin-configuration with the lowest energy needs to be found, since the system will go to this configuration. To find the minimal energy, the LLG-equation, given by formula 10 needs to be solved.

$$\dot{\mathbf{S}}_{ij}^1 = -\frac{1}{1+\alpha^2}\mathbf{S}_{ij}^1 \times \mathbf{H}_{ij}^{\text{eff}} - \frac{\alpha}{1+\alpha^2}\mathbf{S}_{ij}^1 \times \mathbf{S}_{ij}^1 \times \mathbf{H}_{ij}^{\text{eff}} \quad (22)$$

This is a differential equation for the spin at every lattice point and is evaluated for the x-, y- and z-components of the spin individually.

So to get the spin-configuration the differential equation of the form $\dot{\mathbf{S}}_{ij}^1 = F(\mathbf{S}_{ij}^1, t)$ needs to be solved. This is done numerically by the Runge-Kutta method. In this method Taylor series are used to solve this equation for every point of time, so the result is a series of configurations, one for every point of time. Only the final configuration is used, since then the energy is minimized. To check whether the Runge-Kutta method worked, the energy is plotted against time.

The final goal is to find the several phases for varying J_{\perp} and B . The easiest way to do this is by roughly determining the several phases and determining the phase transitions, both with the use of the procedure described above. It is important to note that both 1st and 2nd order phase transitions can occur. To find a 1st order phase transition the points, at which the energy of both phases is equal, are investigated. For 2nd order phase transitions points the order parameter is used, since its value is zero at the phase transition. An algorithm which increases, or decreases depending on the situation, both J_{\perp} and H in small steps is used to the transition points. After all phase transitions are determined, the phase-diagram can be composed.

3.2 Phase diagram

As was mentioned before a phase-diagram of the magnetic phases for varying values of J_{\perp} and H is constructed. This phase-diagram is shown in the figure below.

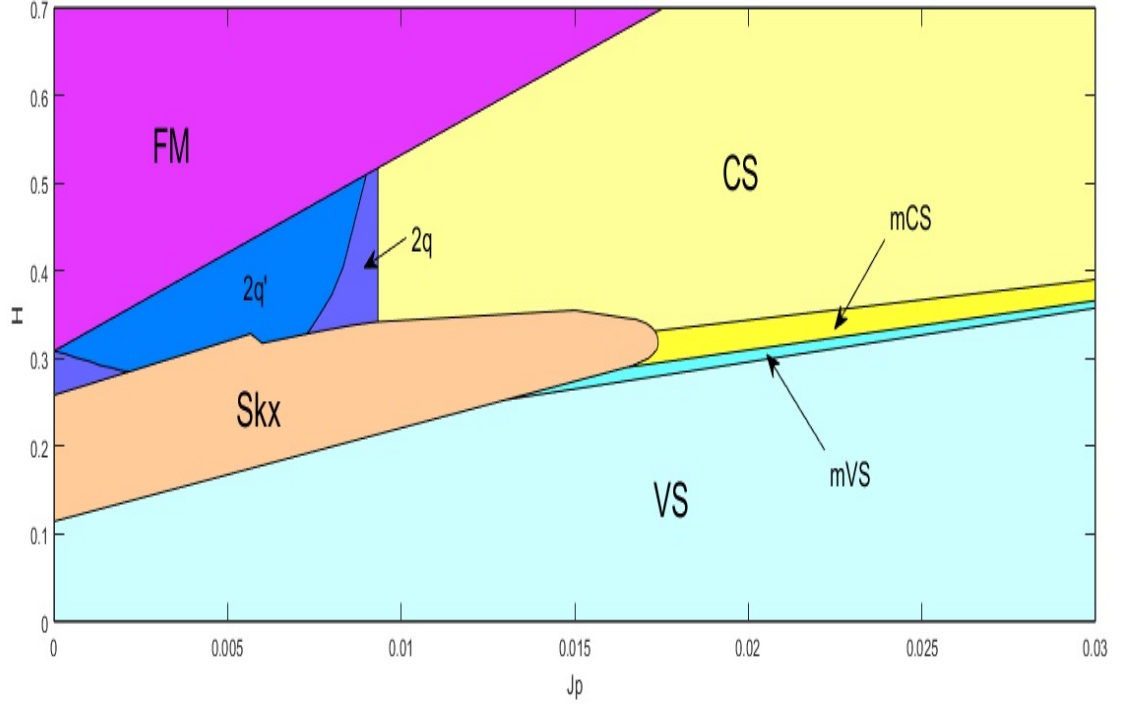


Figure 8: Phasediagram

To clarify this phase-diagram, a remark has to be made about the ground states which are present in this diagram. The best way to describe the different phases is by considering the Fourier series for the spin.[11] The general formula for a Fourier expansion is

$$\mathbf{S}_i = \mathbf{A}_0 + \frac{1}{2} \sum_{n=1}^N \mathbf{A}_n (e^{i\mathbf{q}_n \cdot \mathbf{x}_i} + \phi_n) \quad (23)$$

In this formula i indicates whether S_x , S_y or S_z is considered. In the description of magnetic structures, three wave vectors, \mathbf{q} , are considered. These are the three magnetic modulation vectors which are normal to the external magnetic field and form an angle of $\frac{2\pi}{3}$ with respect to each other. The contribution of higher harmonics is very small. \mathbf{A}_0 is the uniform spin component, since it does not depend on the position and it has only one component, which is parallel to the magnetic field, so in the z -direction. This applies to all possible ground states. \mathbf{A}_n can have contributions to all spin directions.

3.2.1 States

As can be seen in the phase diagram, the ground-state which occupies the lower part of the diagram is the vertical spiral(VS). In the case of the vertical spiral, the spins rotate in a plane which has a nonzero angle with the x-y plane, which is the plane perpendicular to the external magnetic field. In the perfect case it is described by only one \mathbf{A}_n , so \mathbf{A}_2 and \mathbf{A}_3 are zero in all directions. \mathbf{A}_1 is described as follows: $\mathbf{A}_1 = A_1(\text{icos}(\phi), \text{isin}(\phi), 1)$, with ϕ angle with respect to the x-y plane.

When the magnetic field is increased, the vertical spiral picks up some modulations in a direction normal to the spiral plane. So \mathbf{A}_2 and \mathbf{A}_3 become non-zero in the x- and y-direction. This state is called the modulated vertical spiral(mVS).

With further increasing magnetic field, the spins undergo a transition to the conical spiral(CS). In contrast to the vertical spiral, spiral plane does not have an angle with the x-y plane, so it is horizontal. This spiral is also described by only one \mathbf{A}_n , but since the spiral is in the horizontal plane, the z-part of this vector is zero. Furthermore, the spiral is circular, so $\mathbf{A}_1 = A_1(1, \pm i, 0)$ and \mathbf{A}_2 and \mathbf{A}_3 are zero.

The conical spiral can also pick up some modulations under certain circumstances. These modulations can be in all directions, but the modulations for S_x and S_y remain the same. This state is called the modulated conical spiral(mCS).

When J_\perp is reduced, the conical spiral picks up a second spiral which rotates in the opposite direction. So $\mathbf{A}_2 = A_2(1, \mp i, 0)$. Furthermore, a small modulation in the z-direction arises. This state is called the 2q-state. In the special case that $A_2 = A_1$, the state is called the 2q'-state.

When the external magnetic field gets sufficiently large, all spins point in this direction because of the Zeeman-term in the Hamiltonian. So the spin only has a non-zero value in the z-direction. In this case $A_0 = 1$ and all \mathbf{A}_n are zero. This state is of course the well-known ferromagnetic state(FM).

Now the only state left to describe is the skyrmion state(Skx). As was mentioned before in the theory, the skyrmions are defined by their helicity and their vorticity, so these are also used in the Fourier series. A skyrmion state can be seen as 3 vertical spirals rotated with respect to each other by an angle of $\frac{2\pi}{3}$ and these 3 spirals have equal amplitudes. Since the spirals are vertical, the modulations are described with the angle with the z-axis, or the azimuthal angle, which is already given in formula 2. So $\phi = \gamma + m(n-1)\frac{2\pi}{3}$, with γ the helicity and m the vorticity. As was mentioned before, the 3 modulations have the same amplitude, but they don't have the same phase so a $e^{i\chi_n}$ has to be included. The sum of the phases χ_n has to be equal to 0 or to π . So altogether this leads to $\mathbf{A}_n = Ae^{i\chi_n}(\text{icos}(\phi), \text{isin}(\phi), 1)$.

Some of the states are displayed in the following figure.

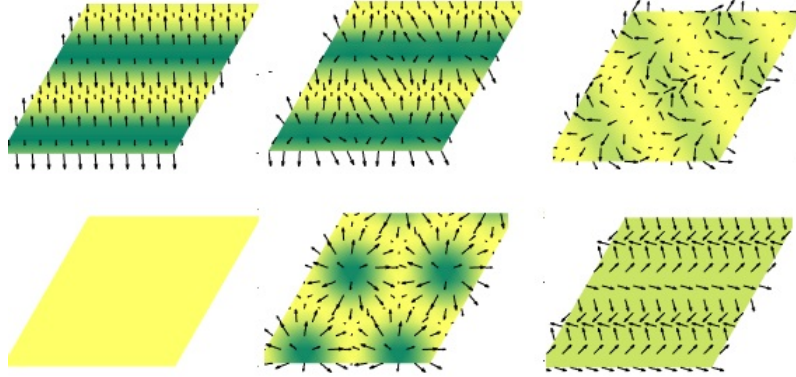


Figure 9: Possible ground-states. The colors indicate the out-of-plane spin. The brighter the higher the value of S_z . The arrows indicate the in-plane spin, so S_x and S_y . From the left top to the right bottom the following states are presented: the vertical spiral, the modulated vertical spiral, the 2q-state, the FM-state, the skyrmion phase and the conical spiral.

3.2.2 Phase transitions

In the phase diagram pictured above, several phase transitions can be seen. The phase transitions can be both continuous and discontinuous. In this section these transitions will be discussed.

The transition between the 2q-state and the FM-state is a continuous one. The 2q-state has 2 modulations, \mathbf{A}_1 and \mathbf{A}_2 , for S_x and S_y . These are the in-plane modulations. Furthermore it has a large A_0 and a small A_3 component in the z-direction. When the external magnetic field is increased, it becomes energetically favorable for the spins to point in the direction of this magnetic field, the z-direction. This is caused by the Zeeman term in the Hamiltonian given in formula 6. The spins start pointing in the z-direction more and more, so the in-plane spin components decrease while the out-of-plane component increases until only the out-of-plane component remains and the FM-state is reached. When the external magnetic field is increased, only the uniform spin component for S_z remains which makes sense since in a FM-state the spin is the same at every position. It can be seen that when J_\perp increases, a larger magnetic field is needed to reach the FM-state. When J_\perp increases, the anti-ferromagnetic interaction between the layers increases. This means that it becomes less favorable to be in the FM-state and a higher magnetic field is needed to get the same effect. For a small region of the 2q-state, both modulations have the same amplitude and the 2q-state becomes a 2q'-state.

The transition between the conical spiral and the FM-state is based on the same mechanism. The only difference is that now the S_x and S_y components of

the spin only have 1 modulation. But again, the in-plane modulation decreases until it completely vanishes and the system is in the FM-state. It can be deduced analytically that the line between the 2q-state and the FM state and the line between the CS-state have the same slope. This is caused by the equivalence of the transitions.

When the anti-ferromagnetic interaction between the layers decreases, the conical spiral acquires a second spiral in a 1st order phase transition and goes to the 2q-state. This second spiral has an opposite orientation with respect to the first spiral, as was already discussed before. Together with this second spiral, the 2q-state gets a small modulation in the z-direction. This modulation in the z-direction makes sure that the energy of the 2q-state is lower than the energy of the conical state in this region. [11]

When the external magnetic field is increased, the vertical spiral transitions to a conical spiral with a first order transition. But first, the vertical spiral gets two sinusoidal modulations and transforms continuously into a modulated vertical spiral. These modulation both only have in-plane components. The same thing happens when the magnetic field is decreased in a conical spiral. The spiral gets extra modulations, however now these modulation are not just in-plane but in every direction. This transition is 2^{nd} order, just as the transition between the VS and the mVS. So actually, there is no transition between the VS-state and the CS-state, but between the mVS-state and the mCS-state.

As mentioned before, this transition is first order, so discontinuous. Both the vertical spiral and the conical spiral only have 1 nonzero A_n , but in the case of the conical spiral A_1^z is also zero. This means that the same thing happens as with the transition to the FM-state described before. Only the uniform component of S_z remains, so S_z is uniform. Furthermore the magnitude of the modulations in the x-direction and the y-direction become equal.

In a significant part of the phase diagram, the vertical spiral does not transform into a conical spiral and the conical spiral does not transform into the 2q-phase. This is the case because in this region the skyrmion phase is the ground state. All transitions between the skyrmion phase and other states are first-order, so discontinuous. As was mentioned before, the skyrmion phase consists of 3 vertical spirals. This means that when the external magnetic field is lowered in the 2q-state and the CS-state, it becomes more and more favorable to get to the skyrmion phase, equivalently to the VS-phase. But this still does not explain why a transition to the skyrmion phase occurs instead of a transition to the vertical spiral. Apparently, for a small region of J_\perp , the skyrmion state becomes energetically favorable with respect to the vertical spiral when the magnetic field is sufficiently strong.

4 Discussion and Conclusion

4.1 Discussion

In the discussion of the results it is important to note that the results for the same kind of model, but with two layers right on top of each other instead of two layers with a shift with respect to each other, were already known. Both phase diagrams are given in appendix D to be able to compare. Even though the results are not necessarily the same, there should be a resemblance. Furthermore the results should be exactly the same if there is no interaction between the layers, so this was a way to check whether the model worked. The biggest difference between the two models is the fact that in the six layer model, each atom has an inter-layer interaction with six other atoms, three in the layer above and three in the layer below, while in the two layer model the atoms only couple to one atom in another layer. So the phase transitions should happen when J_{\perp} has values which are a factor of six smaller, which is also what has been observed.

The lines for the transitions were calculated with an algorithm which gradually increases the values of J_{\perp} and H and solves the LLG-equation for every combination of these values. To check whether these algorithms worked correctly, parts of the phase transitions were also determined by increasing the parameters manually and it was checked whether the same results came out.

To check whether the effective field, used in the LLG-equation, was correct, the derivative of the Hamiltonian was both determined analytically and numerically and the results were compared. The analytical result was used, since this one needs less time to calculate.

Sometimes different starting configurations gave different results for the same values of H and J_{\perp} . In this case, one of the states was the actual groundstate, while the other one was only metastable, which means that it is a stable state even though it does not have the lowest energy. It will only leave this metastable state if a larger impulse is given. To determine what the actual ground state is, the energies have to be compared.

To summarize, because of all the checks it is fair to say that the model works the way it should. However, the determination of the phase transition points is not perfect. This has several reasons.

First of all, the increase of J_{\perp} and H happens in finite steps so it is impossible to determine the phase transition perfectly. Smaller steps make the measurements more accurate, but it also increases the time needed for the calculations so a medium has to be found in this. In most of the cases the increase of J_{\perp} happened in steps of $3,33 * 10^{-4}$ and the increase of H in steps of 0,05, but in some cases smaller steps were necessary.

Different techniques were used for the actual determination of the transition point. In the first order transitions, where the energy difference between the states was considered, this difference was fitted and the roots were determined analytically. However, the energy difference was never perfectly linear, so this gave errors.

In the case of second order transitions, the order parameter was fitted. This

square of this order parameter should have a linear decay. This was the case for the transitions between FM-state and the 2q-state and the transition between the FM-state and the CS-state, but it did not work very well for the transitions between the VS and the CS and their respective modulated versions. The course of the order parameter followed the relation described for a large part, but it broke down near the transition. New calculations with smaller steps were done, but this did not solve the problem. So it was not possible to use this to determine the transition points. Instead, the points were determined manually by using the middle of the interval of the points where the order parameter was zero for the first time and the one before that. This is certainly no ideal determination method, so it gave pretty large errors. This can be seen in appendix B, where the slopes and standard deviations of the transition lines with a linear course are given.

For the transition between the 2q-state and the 2q'-state, which is the special case of the 2q-state with equal amplitudes for the modulation, the difference between the two amplitudes was fitted instead of the energy difference or the order parameter.

In all cases, only the points where either the energy or the order parameter had a regular course were used. In most of the cases enough points could be used, but in some cases only a few points were suitable because of poor choice of J_{\perp} or H .

As was mentioned before in section 3.2.2, the slope of the transition line between the 2q-state and the FM-state and the slope of the transition line between the CS-state and the FM-state should be the same. However, as can be seen in the results, this is not the case. There is a small discrepancy between the slopes, but since the difference is way smaller than the standard deviation, this can be assigned to the flaws in the determination of the transition points, mentioned above.

Furthermore, the transition between the 2q-state and the SkX-state has a peculiar course. The line rises linearly up to $J_{\perp} = 0.0057$, as can be seen in appendix B, then it drops shortly, after which it continues to rise linearly but with a lower slope. Additional measurements with smaller steps were done, but this happened every time.

At last, it has to be noted that the flop phase has not been found in contrast to the two layer model. It was searched for, but it could not be found.

4.2 Conclusion

In conclusion the two layer model of $NiBr_2$, with FM NN interactions, AFM NNN and interlayer interactions, uniaxial anisotropy and an external magnetic field, is improved by increasing the number of layers to six. This is more realistic since the unit cell has three layers and to take the AFM coupling between the layers into account, two unit cells were used. Furthermore, the layers are shifted with respect to each other, in accordance with reality.

When the phase diagrams are compared, it can be concluded that there are a lot of resemblances if one corrects for the fact that in the six layer case

every atom couples to 6 atoms in other layers instead of one in the two layer case. However, there are some minor differences. The biggest difference can be found in the $2q'$ -state, which occupies a way bigger part of the general $2q$ area. Furthermore, the modulated vertical spiral occupies a smaller area. However, it is still fair to say that the outcomes of the two layer model and the six layer model with shift are almost identical. This means that shifting the layers with respect to each other does not make a big impact and neither does increasing the number of layers from two to six.

5 Appendix

5.1 Appendix A: derivation of Landau-Liftshitz-Gilbert equation

The LLG-equation will be derived by considering a free electron in an external magnetic field.[12] The Hamiltonian is given by the Zeeman-term, so we can just use formula 6 but now for just 1 electron:

$$H = -\mathbf{B} \cdot \mu = -\gamma \mathbf{B} \cdot \mathbf{S} \quad (24)$$

with $\mu = \gamma \mathbf{S}$. Now the time-evolution of the spin can be given as follows:

$$\dot{\mathbf{S}} = -\gamma \mathbf{S} \times \mathbf{B} \quad (25)$$

where $[\mathbf{S}_i, \mathbf{S}_j] = i\hbar \mathbf{S}_k$ and $H|\psi\rangle = i\hbar \frac{d}{dt}|\psi\rangle$ are used, with ψ an arbitrary state.

This is the Landau-Liftshitz equation. Gilbert argued that an extra damping term has to be added to compensate for the fact that the magnetization reaches a saturation value, if the external magnetic field gets big enough. At this saturation point, all spins align. The damping term was determined on experimental grounds.

Now the equation can be written as follows:

$$\dot{\mathbf{S}} = -\gamma \mathbf{S} \times \mathbf{B} + \alpha \gamma \mathbf{S} \times \dot{\mathbf{S}} \quad (26)$$

Now, the only thing left is to insert formula 26 for the $\frac{d\mathbf{S}}{dt}$ term and use the fact that the length of the spin-vectors is set to 1, so $S^2 = 1$ and we get:

$$(1 + \alpha^2 \gamma^2) \dot{\mathbf{S}} = -\gamma \mathbf{S} \times \mathbf{B} - \alpha \gamma^2 \mathbf{S} \times \mathbf{S} \times \mathbf{B} \quad (27)$$

The notion has to be made that this derivation only applies to a single electron. To compensate for this fact, the magnetic field is replaced by the effective field. With this replacement and by renaming the parameters, this result is compatible with formula 10.

5.2 Appendix B: Results

In this section the slopes of the transition lines that are assumed linear are given with their corresponding standard deviation.

	Starting point(J_{\perp},H)	ending point (J_{\perp},H)	$\frac{\Delta H}{\Delta J_{\perp}}$	σ
2q-FM	(0,0.309)	(0.00933,0.517)	22.36	1.98
CS-FM	(0.00933,0.515)	(0.0176,0.700)	22.55	2.76
mVS-VS	(0.0133,0.255)	(0.0300,0.358)	6.28	2.36
mCS-CS	(0.0133,0.315)	(0.0300,0.390)	4.59	1.39
mVS-mCS	(0.0133,0.273)	(0.0300,0.368)	5.62	0.50
Skx-2q	(0,0.2641)	(0.0057,0.3282)	11.31	0.22
Skx-VS	(0,0.1144)	(0.0167,0.2915)	10.59	0.38
2q-CS ($\frac{\Delta J_{\perp}}{\Delta H}$)	(0.00933,0.3085)	(0.00933,0.5172)	0.00	0.01

Table 1: slopes of phase transitions

5.3 Appendix C: Phasediagrams of two and six layer model

In this section, both the phasediagram of the two layer model and the six layer model is given in order to be able to compare them.

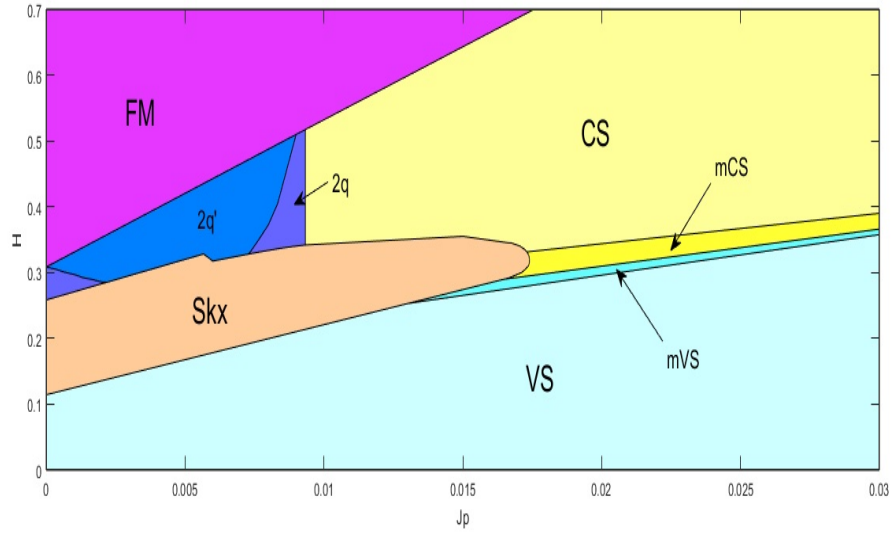


Figure 10: Phasediagram of six layer model.

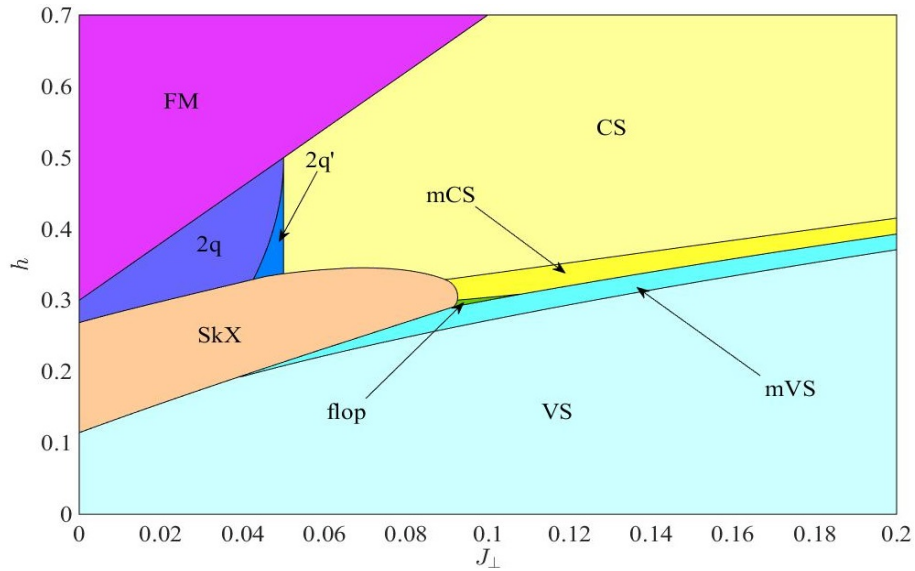


Figure 11: Phasediagram of two layer model.

5.4 Appendix D: Abbreviations

SkX: Skyrmion crystal
LTEM: Lorentz transmission electron microscope.
TMR: tunnel magnetoresistance.
MRAM: magnetoresistive random access memory.
FM: ferromagnet(ic).
AFM: anti-ferromagnet(ic).
DM: Dzyaloshinskii-Moriya.
NN: nearest neighbors.
NNN: next-nearest neighbors.
LLG: Landau-Lifshitz-Gilbert.
CS: conical spiral.
VS: vertical spiral.
mVS: modulated vertical spiral.
mCS: modulated conical spiral.

References

- [1] N. N. . Y. Tokura, “Topological properties and dynamics of magnetic skyrmions,” *Nature Technology*, december 2013.
- [2] A. N. . C. Pfeleiderer, “Topological hall effect in the a phase of mnsi,” *Physics Review Letters*, may 2009.
- [3] S. S. . M. Mochizuki, *Skyrmions in magnetic materials*, 2016.
- [4] G. P. Z. Xichao Zhang, “Skyrmion-skyrmion and skyrmion-edge repulsions in skyrmion-based racetrack memory,” *Scientific reports*, january 2015.
- [5] S. R. A. T. . A. F. J. Sampaio, V. Cros, “Nucleation, stability and current-induced motion of isolated magnetic skyrmions in nanostructures,” *Nature Nanotechnology*, september 2013.
- [6] B. van Dijk, *Skyrmions and the Dzyaloshinskii-Moriya interaction*, december 2014.
- [7] A. P. . A.Zvezdin, “Dzyaloshinskii-moriya-type interaction and lifshitz invariant in rashba 2d electron gas systems,” *A letters journal exploring the frontiers of physics*, september 2014.
- [8] L.Landau, “On the theory of phase transitions,” *Zh. Eksp. Teor. Fiz.*, 1937.
- [9] A.Sparavigna, “On the role of lifshitz invariants in liquid crystals,” *Materials*, november 2007.
- [10] A. Ramirez, “Geometrically frustrated matter-magnets to molecules,” *Material Research Society*, june 2005.
- [11] A. L. . M. Mostovoy, “Multiply periodic states and isolated skyrmions in an anisotropic frustrated magnet,” *Nature Communications*, january 2015.
- [12] M.Lakshmanan, “The fascinating world of landau-lifshitz-gilbert equation: an overview,” *Philosophical transactions of the Royal Society*, january 2011.